

## RESEARCH ARTICLE

# Development of fluorescent peptide G protein-coupled receptor activation biosensors for NanoBRET characterization of intracellular allosteric modulators

James P. Farmer<sup>1,2</sup>  | Shailesh N. Mistry<sup>3</sup>  | Charles A. Laughton<sup>3</sup>  |  
Nicholas D. Holliday<sup>1,4</sup> 

<sup>1</sup>School of Life Sciences, The Medical School, Queen's Medical Centre, University of Nottingham, Nottingham, UK

<sup>2</sup>Centre of Membrane Proteins and Receptors, University of Birmingham and University of Nottingham, Nottingham, UK

<sup>3</sup>School of Pharmacy, University of Nottingham, Nottingham, UK

<sup>4</sup>Excellerate Bioscience, Biocity, Nottingham, UK

## Correspondence

James P. Farmer and Nicholas Holliday, School of Life Sciences, The Medical School, Queen's Medical Centre, University of Nottingham, Nottingham NG7 2UH, UK.

Email: [mbyjf3@nottingham.ac.uk](mailto:mbyjf3@nottingham.ac.uk) and [mbzndh@nottingham.ac.uk](mailto:mbzndh@nottingham.ac.uk)

## Funding information

British Pharmacological Society (BPS)

## Abstract

G protein-coupled receptors (GPCRs) are widely therapeutically targeted, and recent advances in allosteric modulator development at these receptors offer further potential for exploitation. Intracellular allosteric modulators (IAM) represent a class of ligands that bind to the receptor–effector interface (e.g., G protein) and inhibit agonist responses noncompetitively. This potentially offers greater selectivity between receptor subtypes compared to classical orthosteric ligands. However, while examples of IAM ligands are well described, a more general methodology for assessing compound interactions at the IAM site is lacking. Here, fluorescent labeled peptides based on the G $\alpha$  peptide C terminus are developed as novel binding and activation biosensors for the GPCR-IAM site. In TR-FRET binding studies, unlabeled peptides derived from the G $\alpha$ s subunit were first characterized for their ability to positively modulate agonist affinity at the  $\beta_2$ -adrenoceptor. On this basis, a tetramethylrhodamine (TMR) labeled tracer was synthesized based on the 19 amino acid G $\alpha$ s peptide (TMR-G $\alpha$ s19cha18, where cha = cyclohexylalanine). Using NanoBRET technology to detect binding, TMR-G $\alpha$ s19cha18 was recruited to Gs coupled  $\beta_2$ -adrenoceptor and EP<sub>2</sub> receptors in an agonist-dependent manner, but not the Gi-coupled CXCR2 receptor. Moreover, NanoBRET competition binding assays using TMR-G $\alpha$ s19cha18 enabled direct assessment of the affinity of unlabeled ligands for  $\beta_2$ -adrenoceptor IAM site. Thus, the NanoBRET platform using fluorescent-labeled G protein peptide mimetics offers novel potential for medium-throughput screens to identify IAMs, applicable across GPCRs coupled to a G protein class. Using the same platform, Gs peptide biosensors also represent useful tools to probe orthosteric agonist efficacy and the dynamics of receptor activation.

**Abbreviations:** BRET, Bioluminescence resonance energy transfer; CHA, Cyclohexylalanine; GPCR, G protein-coupled receptor; HTRF, Homogeneous time-resolved fluorescence; Nluc, Nanoluc Nanoluciferase; ss, SNAPtag; TM, Transmembrane region; TMR, Tetramethylrhodamine; TR-FRET, Time-resolved Förster Resonance Energy Transfer;  $\beta_2$ -AR,  $\beta_2$ -Adrenoceptor.

This is an open access article under the terms of the [Creative Commons Attribution-NonCommercial-NoDerivs](https://creativecommons.org/licenses/by-nc-nd/4.0/) License, which permits use and distribution in any medium, provided the original work is properly cited, the use is non-commercial and no modifications or adaptations are made.

© 2022 The Authors. *The FASEB Journal* published by Wiley Periodicals LLC on behalf of Federation of American Societies for Experimental Biology.

## KEYWORDS

 $\beta$ 2-Adrenoceptor, Allosteric modulators, Biosensors, CXCR2, GPCRs, Prostanoid receptor EP<sub>2</sub>

## 1 | INTRODUCTION

G protein-coupled receptors (GPCRs) are the largest family of membrane-bound receptors and, with over 27% of the global market share for therapeutic drugs, continue to be the most clinically targeted among receptor superfamilies.<sup>1</sup> Within the GPCR superfamily, the class A rhodopsin like receptors are most numerous (approximately 350 members) and are grouped by conservation of key amino acid motifs supporting the seven transmembrane helical bundle structure and conformational changes on activation.<sup>1</sup> Classical GPCR signaling involves the formation of an agonist–receptor–effector complex (the allosteric ternary complex<sup>2</sup>) to activate heterotrimeric G proteins (or other signaling proteins, such as  $\beta$ -arrestins). Class A GPCRs primarily signal through G $\alpha$ s, G $\alpha$ i/o, G $\alpha$ q/11, or G $\alpha$ 12/13 containing G proteins, each with distinct functional outcomes including cAMP and calcium mobilization, modulation of ion channel activity, and protein kinase cascades and gene expression.<sup>3,4,5,6</sup> A key component of the interaction between the activated GPCR and the G $\alpha$  subunit is determined by the G $\alpha$  C terminus (the  $\alpha$ 5 helix), which engages the GPCR intracellular domain in a cleft between helices TM3 and TM5.<sup>2,7–9</sup> The sequence of the G $\alpha$   $\alpha$ 5 helix is an important driver determining the selectivity of GPCR interaction with different G $\alpha$  classes; its selective interaction with the active agonist-bound receptor conformation provides the basis for the ternary complex and allosteric stabilization of agonist high affinity binding to the receptor in the presence of the G protein.<sup>6</sup>

The nature of the GPCR–G protein interaction pocket provides opportunity for small molecule intervention to modulate receptor function, distinctive from classical targeting of the orthosteric binding site. Indeed, high-affinity intracellular allosteric modulators (IAMs) have been reported that act as noncompetitive antagonists to prevent signaling, for a range of G<sub>i</sub> and G<sub>s</sub> coupled receptors including the chemokine receptors CCR2, CXCR2, CCR5, and CCR9; the  $\beta$ <sub>2</sub>-adrenoceptor ( $\beta$ <sub>2</sub>-AR); and most recently the prostanoid receptor EP<sub>2</sub>.<sup>8,10–14</sup> In line with other approaches to develop allosteric GPCR ligands,<sup>8,15</sup> the rationale for IAM development includes the ability to develop selective ligands against receptor subtypes with conserved orthosteric binding sites, or ones which are multifaceted and complex for small molecule design (e.g., chemokines). Intracellular allosteric modulation may also give rise to useful pharmacological properties, for example, an IAM series at the EP<sub>2</sub> prostanoid receptor displayed use dependence (where the functional effect of the modulator is enhanced

in the presence of the endogenous agonist)—this can arise from a higher affinity for the activated agonist–GPCR conformation, while maintaining blockade of receptor–effector coupling.<sup>14</sup> However, to date, a general target methodology is lacking for identifying novel IAMs by their affinity for the target GPCR–G protein interface.

Early influential studies to explore the receptor–G protein coupling mechanism demonstrated the particular role of the G $\alpha$  C terminal  $\alpha$ 5 helix through the use of peptide mimetics or expressed mini-genes, showing their ability to compete with native G protein binding and inhibit GPCR signaling depending on their sequence.<sup>16–20</sup> However, further exploitation of these peptides as tools was initially limited by relatively modest affinity, ways to assess the direct engagement of the peptides with the receptor, and issues such as lack of cell permeability for functional studies. Recently, Mannes et al.<sup>21</sup> have identified a number of modifications to G $\alpha$ s C terminal peptides capable of improving affinity for the  $\beta$ <sub>2</sub>-adrenoceptor, and also demonstrating their use-dependent properties in which the high agonist affinity active conformation of the GPCR was selectively stabilized. Given that activity was preserved at another G<sub>s</sub>-coupled GPCR (the D1 dopamine receptor),<sup>21</sup> these peptides therefore offer starting points for broad selectivity tool development for assessing GsPCR IAM binding sites.

Increasingly, the use of fluorescent ligands and resonance energy transfer technologies (such as TR-FRET and NanoBRET) provides an attractive alternative to radioligand and other approaches to assess binding in both GPCR mechanism of action studies and compound screening.<sup>22–26</sup> The selectivity of the resonance energy transfer signal (constrained to a distance of less than 10 nm between the donor luciferase/fluorophore and acceptor fluorescent tracer) enables these assays to be performed in a homogeneous format (without separation of the free fluorescent ligand) and accurate determination of ligand binding even at high tracer concentrations. In this study, we demonstrate a novel generally applicable NanoBRET approach to monitor the binding of ligands at GPCR IAM sites, to quantify interactions between inactive GPCRs and a fluorescent derivative of the 19 amino acid G $\alpha$ s C terminal peptide G $\alpha$ s19cha18 (where cha = cyclohexylalanine).<sup>21</sup> Supported by assessments at both the  $\beta$ <sub>2</sub>-adrenoceptor and EP<sub>2</sub> prostanoid receptor, we show how this provides a sensitive real-time biosensor for receptor activation by agonists of differing efficacy, and generally applicable binding assay for the determination of the ligand affinity at the GPCR–G protein IAM binding site.

## 2 | MATERIALS AND METHODS

### 2.1 | Materials

G $\alpha$  C terminal peptides were purchased from GenScript Biotech (New Jersey, USA) (4 mg, >95% purity) and stored at  $-20^{\circ}\text{C}$  at a 10-mM stock concentration in DMSO prior to use (sequences given Table 1). General molecular biology enzymes were obtained from Fermentas (ThermoFisher Scientific, Loughborough, UK), and other molecular biology consumables were from Sigma-Aldrich (Poole, UK) or ThermoFisher (Loughborough, UK) unless otherwise stated.

All assay plates used were OptiPlate-384 white well microplates (product number: 6007290, PerkinElmer LAS Ltd, UK) unless otherwise stated. BODIPY-FL-PEG8-(S)-Propranolol was purchased from Hello Bio Ltd (CA200693,<sup>27</sup> Bristol, UK) and all other compounds were purchased from ThermoFisher (Loughborough, UK) and stored as 10 mM stocks in DMSO at  $-20^{\circ}\text{C}$  unless otherwise stated. The nanoluciferase substrate furimazine was purchased from Promega Biotech (Madison, USA).

### 2.2 | Cell culture

HEK 293 cell lines were transfected with cDNAs encoding (i) N-terminal SNAP-tagged human  $\beta_2$ -adrenoceptor (Hek-ss $\beta_2$ -AR, Genbank: NM\_000024), as described in Valentin-Hansen et al.<sup>28</sup> or (ii) SNAP-tagged human  $\beta_2$ -adrenoceptor or human EP<sub>2</sub> receptors fused at the C terminus to a thermostable Nanoluciferase (Hek-ss $\beta_2$ -AR/EP<sub>2</sub>-tsNluc) using Lipofectamine 3000 reagent (Invitrogen, Paisley, UK). Original SNAP tag and nanoluciferase sequences were from NEB (Hitchin UK) and Promega (Southampton UK), respectively. The tsNluc contains structural stabilizing Nluc substitutions as described in Hoare et al.<sup>29,30</sup> Stable mixed population cell lines were established through G418 resistance (encoded by the plasmid vector (pcDNA3.1 neo<sup>+</sup>, Invitrogen, Paisley UK). Cells were maintained in Dulbecco's modified Eagle's medium (Sigma-Aldrich,

TABLE 1 Amino acid sequences of G $\alpha$  C terminal peptides used in this study

G $\alpha$ C-terminal peptide	Amino acid sequence (N–C terminus left to right)
G $\alpha$ s11	QRMHLR QYELL
G $\alpha$ s24	NIRRVFNDCRDII QRMHLRQYELL
G $\alpha$ s19cha18	FNDCRDII QRMHLRQYE{CHA}L
TMR-G $\alpha$ s19cha18	<b>TMR</b> -FNDCRDII QRMHLRQYE{CHA}L
G $\alpha$ i24	NVQVFVDAVTDVI IKNNLKDCLF

Note: {CHA} indicates cyclohexylalanine, **TMR** indicates N terminal incorporation of Tetramethylrhodamine.

Poole, UK) supplemented with glucose (4.5 g/L), 0.2 mg/ml G418, L-Glutamine (4.5 g/L) and with 10% fetal calf serum (Life Technologies, Paisley, U.K.)

### 2.3 | Terbium labeling of SNAP-tagged human $\beta_2$ -adrenoceptors and membrane preparations

For TR-FRET assays requiring terbium (Tb) labeling, cell culture medium was removed from T-175 cm<sup>2</sup> flasks containing confluent adherent Hek-ss $\beta_2$ -AR and replaced with 10 ml Tag-lite medium (LABMED, Cisbio Bioassays) containing 100 nM SNAP-Lumi4-Tb (Cisbio Bioassays, Bagnols-sur-Ce'ze, France). Cells were then incubated in labeling medium for 1 h at  $37^{\circ}\text{C}$  under 5% CO<sub>2</sub>. For membrane preparations, Tb-labeled Hek-ss $\beta_2$ -AR cells and unlabeled Hek-ss $\beta_2$ -AR-tsNluc, HEK-EP<sub>2</sub>-tsNluc, or HEK-ssCXCR2-tsNluc cells were washed twice with phosphate-buffered saline (PBS, Sigma-Aldrich, Pool, UK) to remove excess labeling or growth medium before being removed by scraping into 10 ml PBS. Detached cells were then collected and pelleted by centrifugation (10 min, 2000 rpm) and pellets were frozen at  $-80^{\circ}\text{C}$ , until required. For membrane homogenization (all steps at  $4^{\circ}\text{C}$ ), 20 ml wash buffer (10 mM HEPES, 10 mM EDTA, pH: 7.4) was added to the pellet before disruption (eight bursts) with an Ultra-Turrax homogenizer (Ika-Werk GmbH & Co. KG, Staufen, Germany), and subsequently centrifugation at 48 000 g at  $4^{\circ}\text{C}$ . Supernatant was discarded and the pellet was resuspended in 20 ml wash buffer and centrifuged again as above. The final pellet was suspended in cold 10 mM HEPES with 0.1 mM EDTA (pH 7.4). Protein concentration was determined using the bicinchoninic acid assay kit (Sigma-Aldrich, Pool, UK) using bovine serum albumin as standard, and aliquots were maintained at  $-80^{\circ}\text{C}$  until required.

### 2.4 | TR-FRET BODIPY-FL-PEG8-(S)-Propranolol binding assays to determine association kinetics and equilibrium ligand binding

TR-FRET binding assays were performed using low sodium assay binding buffer (25 mM HEPES, 1% DMSO, 0.1 mg/ml Saponin, 0.02% w/v Pluronic acid F127, 1 mM MgCl<sub>2</sub>, and 0.2% BSA (pH 7.4), at  $37^{\circ}\text{C}$  in 384-well Optiplates. To determine fluorescent ligand association kinetics, incubations were performed with BODIPY-FL-PEG8-(S)-Propranolol (FL-propranolol) at varied final assay concentrations (1.56–100 nM) in the absence and presence of 10  $\mu\text{M}$  ICI118551 to determine nonspecific binding. Binding was initiated by the addition of Hek-ss $\beta_2$ -AR cell membranes (1  $\mu\text{g}$ /well) in

assay buffer to a final assay volume of 30  $\mu$ l, performed by online injection on a BMG PHERAstar FSX plate reader (BMG Labtech, Offenburg, Germany). The TR-FRET ratio was then recorded at 10-s intervals, over a 30-min period, on the PHERAstar using 337 nm excitation of the Terbium donor and monitoring donor emission at 490 nm, and acceptor FL-propranolol emission at 520 nm.

For TR-FRET competition binding studies in the same system, assays were performed using the same buffer and temperature conditions above, using 20 nM FL-propranolol tracer in the absence and presence of 14 competing concentrations of unlabeled test orthosteric ligands (salbutamol, isoproterenol, formoterol, and ICI118551), with or without 10  $\mu$ M G $\alpha$  C terminal peptide (G $\alpha$ s11, G $\alpha$ s24, G $\alpha$ s19cha18, or G $\alpha$ i24; Table 1). Binding was initiated by online addition of the Hek-ss $\beta_2$ -AR cell membranes (1  $\mu$ g/well) to a final assay volume of 40  $\mu$ l. Endpoint HTRF readings were taken at 30–120 min time points using the PHERAstar HTRF settings to monitor progress to equilibrium. For these studies, total binding was determined by using assay buffer in the place of competing ligand and NSB was determined with 10  $\mu$ M ICI118551. For studies exploring the effect of GTP-analogs on agonist affinity, 100  $\mu$ M Guanosine 5'-[ $\beta$ , $\gamma$ -imido] triphosphate (Gpp(NH)p, Sigma Aldrich, Pool, UK) was included within the assay buffer.

## 2.5 | Bioluminescence resonance energy transfer (NanoBRET) assays to monitor fluorescent G protein peptide recruitment

NanoBRET assays used either low sodium assay binding buffer as described for TR-FRET binding measurements or an extracellular Hank's balanced saline solution (136 mM NaCl, 5.1 mM KCl, 0.44 mM KH<sub>2</sub>PO<sub>4</sub>, 4.17 mM NaHCO<sub>3</sub>, 0.34 mM Na<sub>2</sub>HPO<sub>4</sub>, 1% DMSO, 0.1 mg/ml Saponin, 0.02% Pluronic acid F<sub>127</sub>, 0.2% BSA, and 20 mM HEPES, pH 7.4), as indicated in the text. TMR-G $\alpha$ s19cha18 binding was first characterized by addition of varying fluorescent probe concentrations (8–1000 nM) to 1  $\mu$ g/well Hek-ss $\beta_2$ -AR-tsNluc cell membranes, in which donor luciferase luminescence was stimulated with the addition of furimazine (1/960 dilution from Promega manufacturer's stock) in the additional absence or presence of the orthosteric agonist 10  $\mu$ M isoproterenol (final assay volume, 40  $\mu$ l). Fluorescent peptide NSB was defined by the inclusion of 10  $\mu$ M unlabeled G $\alpha$ s19cha18 peptide. Endpoint reads at 30- and 60-min incubation at 37°C were taken on the PHERAstar as the BRET ratio between donor luminescence (450 nm emission) and acceptor TMR-G $\alpha$ s19cha18 fluorescence (550 nm) to determine TMR-G $\alpha$ s19cha18 binding.

For quantitative analysis of TMR-G $\alpha$ s19cha18 recruitment by orthosteric agonists, 500 nM TMR-G $\alpha$ s19cha18

was incubated with 1  $\mu$ g/well Hek-ss $\beta_2$ -AR-tsNluc cell membranes, 1/960 dilution furimazine, and the following ligands at the indicated final concentrations: salbutamol, salmeterol, isoproterenol, formoterol, or ICI118551. To initiate the recruitment, membranes were separately preincubated (5 min) with furimazine to establish luminescence output, prior to their online injection using the PHERAstar to assay buffer containing the probe peptide and stimulating ligands. NanoBRET was monitored for 30 min every 1.16 min on the PHERAstar, using the BRET ratiometric measurements described above. In experiments to understand TMR-G $\alpha$ s19cha18 selectivity, agonist binding assays were repeated using the same protocol employing Hek-EP<sub>2</sub>-tsNluc or Hek-ssCXCR2-tsNluc cell membranes, stimulated with PGE<sub>2</sub><sup>9</sup> or CXCL8 (Strattech Scientific, Cambridge, UK), or vehicle. In these experiments, the extent of recruitment was assessed 30 min after membrane addition at 37°C.

To determine unlabeled ligand affinities using competition binding, assays employed 500 or 125 nM TMR-G $\alpha$ s19cha18, a range of competing concentrations of unlabeled peptides (e.g., G $\alpha$ s19cha18, G $\alpha$ s24, G $\alpha$ s11, or G $\alpha$ i24), the inclusion of 10  $\mu$ M isoproterenol and 1  $\mu$ g/well Hek-ss $\beta_2$ -AR-tsNluc cell membranes pre-incubated with 1/960 dilution of furimazine as indicated above (final volume, 50  $\mu$ l). Incubations were performed at 37°C and BRET measurements were taken every 30 min over a 2-h interval, using PHERAstar (550 nm/450 nm ratio).

## 2.6 | Data analysis

TR-FRET and NanoBRET data were performed in either triplicate or duplicate unless otherwise indicated and were routinely expressed as the respective acceptor/donor emission ratios (520 nm/490 nm  $\times$  1000 for TR-FRET; 550 nm/450 nm for NanoBRET). In competition binding studies, individual experiment data were normalized to total specific binding in the absence of competing ligands (100%), while in agonist-stimulated recruitment measurements, data were normalized to a maximal concentration of stimulating reference agonist.

For TR-FRET FL-propranolol association kinetic data, specific binding traces for FL-propranolol (defined as total binding—NSB) were fitted to a one site association model. Global fitting of this model across multiple fluorescent ligand concentrations from the same experiment enabled estimation of FL-propranolol association ( $k_{on}$ ) and dissociation rate constants ( $k_{off}$ ), together with the kinetically derived  $K_D$  ( $= k_{off}/k_{on}$ ) using the equations:

$$Bound = B_{plateau} \cdot (1 - e^{-k_{obs} \cdot t})$$

where the  $B_{\text{plateau}}$  is the equilibrium level of tracer binding and the observed association rate constant  $k_{\text{obs}}$  is related to the binding rate constants for FL-propranolol in a single site model by:

$$k_{\text{obs}} = [\text{FL\_propranolol}] \cdot k_{\text{on}} + k_{\text{off}}$$

Endpoint saturation analysis also enabled the calculation of the equilibrium dissociation constant ( $K_{\text{D}}$ ) for fluorescent tracer, as well as total binding density as  $B_{\text{max}}$  in TR-FRET and BRET experiments, based on:

$$\text{Specific binding} = B_{\text{max}} \cdot \frac{[\text{Tracer}]}{[\text{Tracer}] + K_{\text{D}}}$$

Competition binding studies were fitted to determine competing ligand  $\text{IC}_{50}$  concentrations, using a four-parameter fit including the Hill slope ( $n$ )

$$\text{Specific binding} = \text{Basal} + \frac{\text{Total Specific binding} \cdot \text{IC}_{50}^n}{[\text{Ligand}]^n + \text{IC}_{50}^n}$$

where appropriate, the Cheng–Prusoff equation was applied to convert  $\text{IC}_{50}$  estimates to the competing ligand dissociation constant as  $K_i$

$$K_i = \frac{\text{IC}_{50}}{1 + \frac{[\text{FL}]}{K_{\text{FL}}}}$$

$K_{\text{FL}}$  and  $[\text{FL}]$  represent the fluorescent probe dissociation constant and concentration, respectively.

For endpoint agonist stimulation of TMR-G $\alpha$ s19cha18 recruitment measured by NanoBRET, concentration response curve analysis was performed to obtain the estimates of ligand potency ( $\text{EC}_{50}$ ) and maximal response  $R_{\text{max}}$ :

$$\text{Response} = \text{Basal} + R_{\text{max}} \cdot \frac{[\text{Agonist}]^n}{[\text{Agonist}]^n + \text{EC}_{50}^n}$$

Alternatively kinetic Gs recruitment data were fitted to a rise to steady-state model, as described by Hoare et al.<sup>27</sup>:

$$\text{Response (at time } t) = \text{Basal} + \text{Response}_{\text{steady state}} \cdot (1 - e^{-k_{\text{obs}} \cdot t})$$

$$\text{Initial rate} = k_{\text{obs}} \cdot \text{Response}_{\text{steady state}}$$

In this analysis, concentration response data were analyzed by defining the initial rate at each ligand concentration as the response.

All data analysis was performed using Prism 9.0 (GraphPad Software, San Diego). Parameter estimates were expressed as pX ( $-\log X$ ) where appropriate (e.g.,  $\text{pEC}_{50}$ ) and data from individual experiments were pooled as mean  $\pm$  SEM. Statistical significance between two data groups was assessed by Student's unpaired or paired  $t$ -test as indicated in the text, with a level of significance defined as  $p < .05$ .

### 3 | RESULTS

#### 3.1 | Determination of the effects of G $\alpha$ s C terminal peptides on $\beta_2$ -adrenoceptor ligand binding using the BODIPY-FL-PEG8-(S)-Propranolol TR-FRET binding assay

In order to probe the potential allosteric modulatory effects of different G $\alpha$  C terminal peptides on  $\beta_2$ -adrenoceptor ( $\beta_2$ -AR), we first established a membrane TR-FRET binding assay using terbium labeled HEK ss $\beta_2$ -AR membranes and the fluorescent antagonist tracer FL-propranolol.<sup>24,31,32</sup> The binding parameters of FL-propranolol were determined through the analysis of the association kinetics for the fluorescent tracer (Figure S1), confirming single-site behavior and FL-propranolol estimates for the association rate constant  $k_{\text{on}}$  ( $1.30 \pm 0.18 \times 10^7 \text{ M}^{-1} \text{ min}^{-1}$ ), dissociation rate constant  $k_{\text{off}}$  ( $0.18 \pm 0.02 \text{ min}^{-1}$ ), and a kinetically derived  $K_{\text{D}}$   $16.1 \pm 3.1 \text{ nM}$  ( $n = 5$ ). These estimates are consistent with previously reported data for propranolol at the  $\beta_2$ -AR<sup>33</sup> and the previously published pharmacology for related fluorescent propranolol derivatives.<sup>27</sup>

FL-propranolol competition analysis was then performed to determine the affinities of three representative agonist ligands (isoproterenol, formoterol, salbutamol) and the unlabeled antagonist ICI118551 in a low sodium assay buffer as described in the methods (Figure 1; Table 2)—and to examine the potential allosteric effect of different G $\alpha$ s-derived peptides. Specific binding was monitored at a number of time points (data not shown) to ensure the 2-h endpoint shown represented equilibrium conditions. In the absence of G $\alpha$ s peptides, the measured affinity of these example ligands was as expected from literature data.<sup>31,33</sup> Notably, 10  $\mu\text{M}$  G $\alpha$ s24 and 10  $\mu\text{M}$  G $\alpha$ s19cha18 each promoted a significant increase in measured affinity for the orthosteric agonists (Figures 1 and S2; Table 2). The extent of the shift in affinity was highest for the high efficacy agonists isoproterenol and formoterol and reduced for the lower efficacy agonist salbutamol. In contrast, G $\alpha$ s24 and G $\alpha$ s19cha18 had no effect on the affinity of the antagonist ICI118551. We also observed that a shorter 11 amino acid C terminal G $\alpha$ s11 peptide

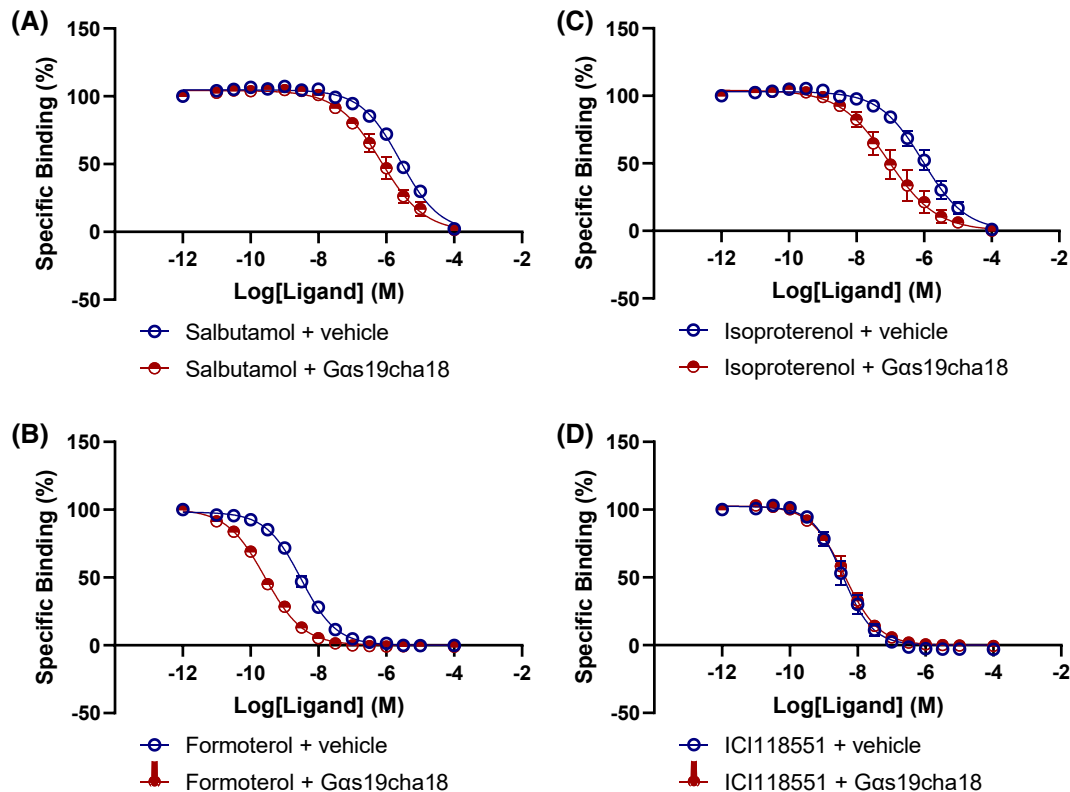


**FIGURE 1** TR-FRET FL-propranolol binding studies in ss $\beta_2$ -AR membranes demonstrate the selective effect of G $\alpha$ s19cha18 (10  $\mu$ M) on agonist affinities. The specific binding data shown were normalized and pooled from five independent experiments, with nonspecific binding determined by addition of 10  $\mu$ M ICI118551. All assays were performed using 20 nM FL-propranolol tracer and low sodium buffer at 37°C for 2 h, with comparator peptide data (G $\alpha$ s24, G $\alpha$ s11) shown in Figures S2 and S4.

**TABLE 2** Binding affinities of  $\beta_2$ -adrenoceptor ligands in the absence and presence of 10  $\mu$ M G $\alpha$ s C terminal peptides

Ligand	G $\alpha$ s24			G $\alpha$ s19cha18		
	Vehicle	10 $\mu$ M peptide	Fold change	Vehicle	10 $\mu$ M peptide	Fold change
Isoproterenol	5.81 $\pm$ 0.17	6.54 $\pm$ 0.19*	5.4	6.18 $\pm$ 0.18	6.93 $\pm$ 0.30**	5.6
Formoterol	8.30 $\pm$ 0.18	8.92 $\pm$ 0.18***	4.2	8.85 $\pm$ 0.07	9.9 $\pm$ 0.08***	11.2
Salbutamol	5.64 $\pm$ 0.12	5.78 $\pm$ 0.22	1.4	5.89 $\pm$ 0.07	6.36 $\pm$ 0.17**	3.0
ICI118551	8.62 $\pm$ 0.12	8.60 $\pm$ 0.12	1.0	8.7 $\pm$ 0.14	8.67 $\pm$ 0.13	0.9

Note: pKi data are presented as mean  $\pm$  SEM and are from five different experiments per peptide, with paired vehicle controls for each peptide. Significant differences between control and peptide assay conditions are indicated by \* $p$  < .05, \*\* $p$  < .01, \*\*\* $p$  < .001 (paired Student's  $t$ -test).

had no effect on orthosteric agonist binding in the same assay, at up to 10  $\mu$ M (Figure S4; Table S1). Finally, we compared the effect of G $\alpha$ s19cha18 on isoprenaline affinity in the membrane binding assay, in the presence and absence of the nonhydrolyzable GTP analog 100  $\mu$ M GppNHp (Figure S3). GppNHp produced an expected decrease in isoprenaline affinity in the assay under control conditions (resulting from disruption of the ternary agonist-receptor-G protein complex in membranes<sup>6</sup>), but the stabilization of a higher affinity isoprenaline-bound receptor state in the presence of G $\alpha$ s19cha18 was unaffected. Taken together, these data supported the binding

of G $\alpha$ s24 and G $\alpha$ s19cha18 to the  $\beta_2$ -AR and their allosteric stabilization of the active conformation selectively promoting high agonist affinity, as previously observed in radioligand binding assays by Mannes et al.<sup>21</sup>

### 3.2 | Establishing a NanoBRET assay to directly monitor TMR-G $\alpha$ s19cha18 recruitment to the $\beta_2$ -Adrenoceptor

The positive enhancement of agonist binding affinity in the  $\beta_2$ -AR was greatest for G $\alpha$ s19cha18, supporting

previous studies indicating the  $\beta_2$ -AR affinity and allosteric modulation by this substituted  $G\alpha s$  peptide.<sup>21</sup> However, this analysis of the effects of the  $G\alpha C$  terminal peptides relied on their indirect allosteric modulation properties, rather than direct demonstration of binding and peptide affinity for the  $\beta_2$ -AR-G protein interaction site. Given the knowledge that the peptide C terminus was likely to make close contact with the  $\alpha 5$ -helix site,<sup>7</sup> we therefore sought to generate a fluorescent probe retaining  $\beta_2$ -AR affinity through N terminal modification of the sequence with the BRET compatible fluorophore tetramethylrhodamine (generating TMR- $G\alpha s19cha18$ ). The ss $\beta_2$ -AR was fused at the C terminus with a thermostable (ts) Nanoluciferase (ss $\beta_2$ -AR-tsNluc) thereby providing a source of intracellularly located donor luminescence and providing opportunity to detect TMR- $G\alpha s19cha18$  to the expressed ss $\beta_2$ -AR-tsNluc in membranes by NanoBRET (Figure 2A).

However, initial saturation studies performed using TMR- $G\alpha s19cha18$  and otherwise unstimulated ss $\beta_2$ -AR-tsNluc membranes (in low sodium buffer used for previous TR-FRET measurements) failed to detect significant specific binding using up to 1  $\mu M$  labeled peptide (Figure 2D). Instead, TMR- $G\alpha s19cha18$  recruitment was only observed in the presence of 10  $\mu M$  isoproterenol, in which a substantive specific BRET measurement was observed that was effectively competed by unlabeled  $G\alpha s19cha18$  peptide (Figure 2B,C). Under these agonist-stimulated conditions and low sodium environment, the TMR- $G\alpha s19cha18$   $K_D$  for the  $\beta_2$ -AR was  $599 \pm 25$  nM (Bmax [as TR-FRET ratio] =  $0.29 \pm 0.05$ ,  $n = 5$ ). The use of an extracellular HBSS-based buffer (with higher sodium concentration) did not significantly affect TMR- $G\alpha s19cha18$  affinity ( $p = .16$ ) or Bmax (Bmax =  $0.21 \pm 0.01$ ,  $p = .20$ ) (Figure S5). These data demonstrated that TMR- $G\alpha s19cha18$  was a suitable probe for the  $\beta_2$ -AR intracellular G protein binding site,

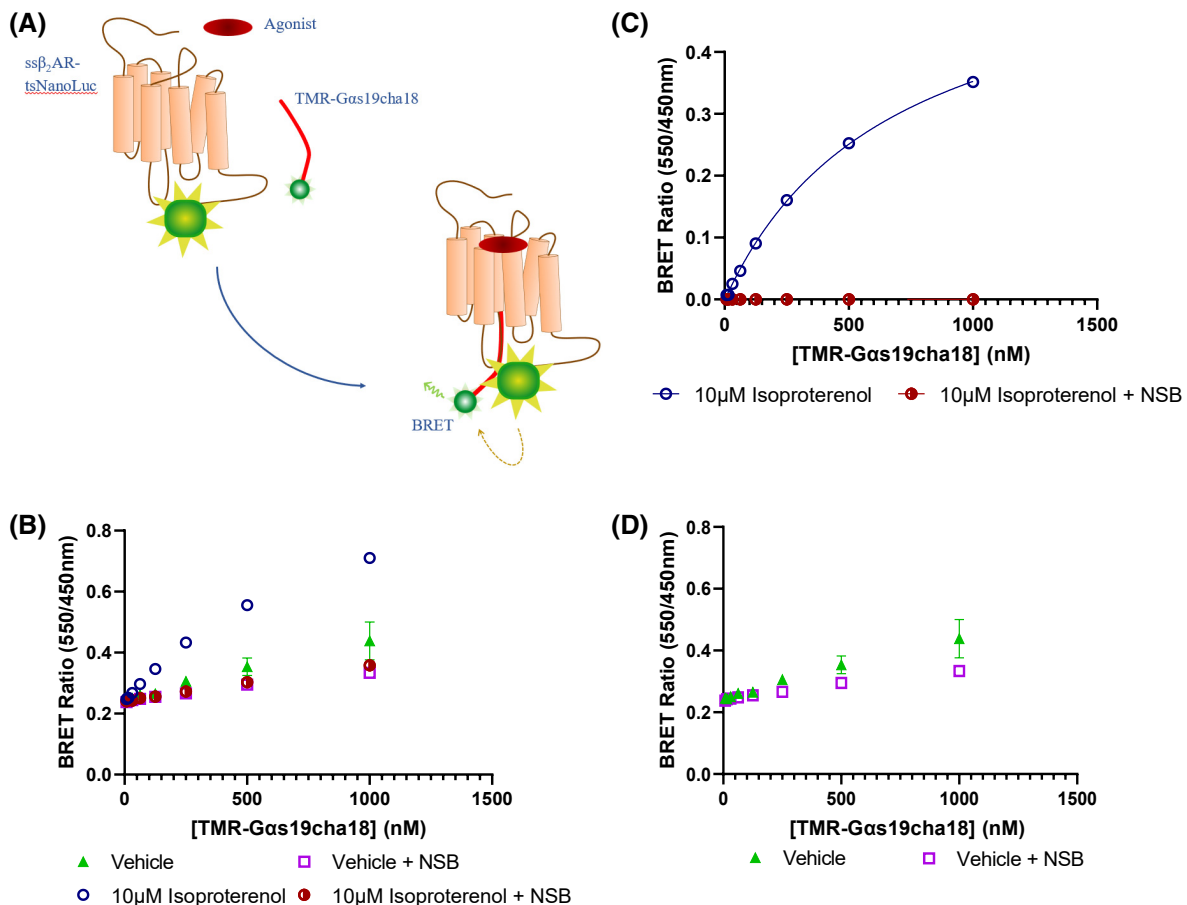


**FIGURE 2** Agonist-dependent binding of TMR- $G\alpha s19cha18$  to the  $\beta_2$ -adrenoceptor determined by NanoBRET. (A) Diagram of TMR- $G\alpha s19cha18$  interaction with ss $\beta_2$ -AR-tsNluc, generating NanoBRET signal, in the presence of an agonist. (B) Saturation binding of TMR- $G\alpha s19cha18$ , demonstrating the increased specific binding observed in the presence of 10  $\mu M$  isoproterenol. (C) Specific binding data in the presence of isoproterenol fitted with a one-site specific binding model to determine TMR- $G\alpha s19cha18$  affinity ( $K_D$ ). (D) Saturation binding measurements for TMR- $G\alpha s19cha18$  to ss $\beta_2$ -AR-tsNluc membranes in an agonist-free environment and low sodium buffer. In B and D, total and nonspecific binding (NSB) were defined by the absence and presence of 10  $\mu M$  unlabeled  $G\alpha s19cha18$ . Data shown are single examples from five independent experiments.

whose binding could be detected by NanoBRET, and appeared dependent on the active receptor conformation promoted by orthosteric  $\beta_2$ -AR agonists.

### 3.3 | $\beta_2$ -Adrenoceptor ligand pharmacology revealed by TMR-G $\alpha$ s19cha18 NanoBRET recruitment assays

Given the agonist dependence of TMR-G $\alpha$ s19cha18 recruitment, we explored the ability of this NanoBRET assay to function as a  $\beta_2$ -AR activation sensor for ligands of known differences in efficacy. Using 500 nM TMR-G $\alpha$ s19cha18 tracer, kinetic and endpoint NanoBRET measurements were performed in ss $\beta_2$ -AR-tsNluc membranes in response to agonists and antagonist, also comparing the low sodium binding buffer initially used with an HBSS-based buffer with higher “extracellular” sodium concentrations. Endpoint concentration response data (Figure 3; Table 3) clearly ranked the agonists isoproterenol, formoterol, salbutamol, and salmeterol in the expected order of potency and maximal response,<sup>31</sup> with salbutamol and salmeterol both identified as partial agonists relative to isoproterenol. The effect of HBSS buffer environment, containing higher sodium concentration, was a reduction in agonist potency (Figure 3B, Table 3). A further advantage of the NanoBRET methodology was the homogeneous assay format and the

ability to collect the kinetics of TMR-G $\alpha$ s19cha18 recruitment for the different agonists over time (Figure 4). Fitting the rise to steady state observed in the data enabled calculation of the initial rate of fluorescent G peptide probe recruitment at each agonist concentration,<sup>34</sup> and to construct concentration–initial response rate relationships for the agonists as shown in Figure 4D, Table 4. These data provided equivalent agonist potency and maximal response measurements to the endpoint concentration–response measurements performed under the same buffer conditions.

### 3.4 | TMR-G $\alpha$ s19cha18 is selective for Gs-coupled receptors

NanoBRET binding assays employing chemokine receptor CXCR2, a Gi selective GPCR, or Gs selective prostanoid receptor EP<sub>2</sub> indicated the selectivity of TMR-G $\alpha$ s19cha18 binding and recruitment for Gs-coupled GPCRs (Figure 5). Stimulation of CXCR2-tsNluc membranes with its chemokine peptide agonist CXCL8 did not increase TMR-G $\alpha$ s19cha18 recruitment above basal levels. Conversely, PGE<sub>2</sub> stimulation of the EP<sub>2</sub>-tsNluc receptor in membranes demonstrated an agonist concentration-dependent increase in TMR-G $\alpha$ s19cha18 NanoBRET (pEC<sub>50</sub> 6.2 ± 0.19, *n* = 3), with levels of specific binding similar to previous  $\beta_2$ -AR responses.

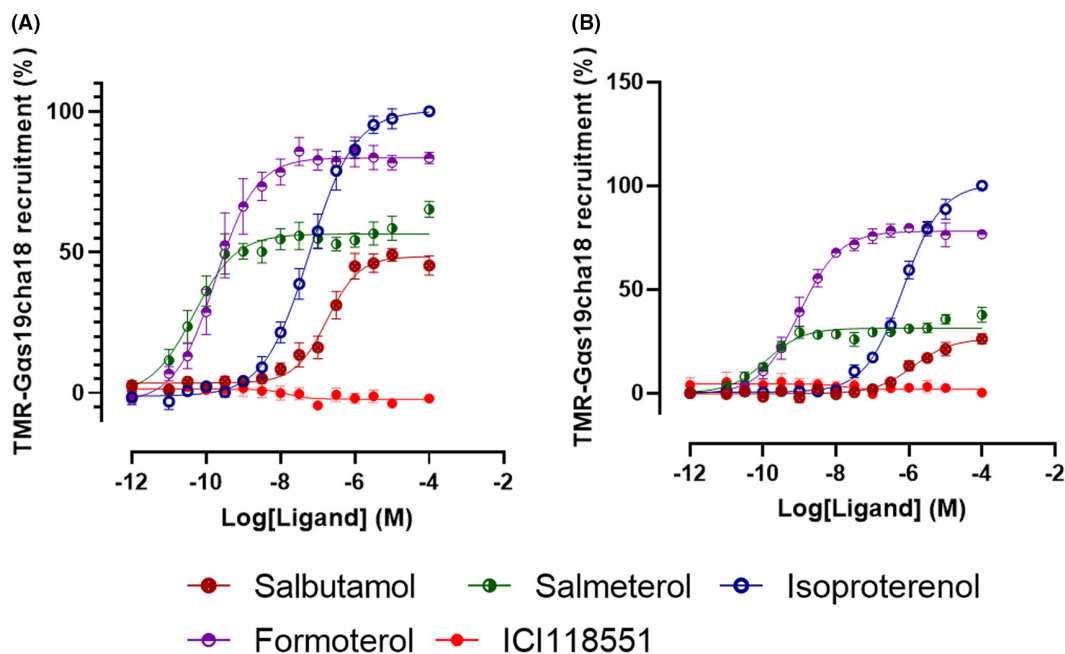


FIGURE 3 Agonist-dependent recruitment of TMR-G $\alpha$ s19cha18 to ss $\beta_2$ -AR-tsNluc measured by NanoBRET. Assays were performed using 500 nM TMR-G $\alpha$ s19cha18 with endpoint binding measured after 30 min, 37°C exposure to different  $\beta_2$ -AR orthosteric ligands, to construct concentration–response relationships. (A and B) represent pooled data from five experiments, performed in low sodium and HBSS buffers, respectively. In each case, agonist responses were normalized to 100  $\mu$ M isoproterenol.



**TABLE 3** Agonist potencies and maximal responses derived from TMR-G $\alpha$ s19cha18 binding in low sodium buffer or extracellular HBSS media

Ligands	Low Sodium		HBSS	
	pEC <sub>50</sub> ± SEM (M)	R <sub>max</sub> ± SEM (%)	pEC <sub>50</sub> ± SEM (M)	R <sub>max</sub> ± SEM (%)
Salbutamol	6.84 ± 0.16	49.2 ± 2.7	5.91 ± 0.22**	26.6 ± 3.4***
Salmeterol	10.32 ± 0.18	57.1 ± 3.5	9.85 ± 0.21	32.4 ± 1.6***
Isoproterenol	7.25 ± 0.12	100.6 ± 1.3	6.15 ± 0.09**	101.1 ± 1.2
Formoterol	9.68 ± 0.18	83.7 ± 3.1	9.02 ± 0.21*	78.0 ± 3.2
ICI118551	–	–3.14 ± 1.6	–	1.50 ± 1.4

Note: Data parameters are presented as mean ± SEM and are from five different experiments per environment. For ICI118551, the effect at 10  $\mu$ M antagonist is recorded as R<sub>max</sub>. Significant differences between pEC<sub>50</sub> or R<sub>max</sub> data in the two buffers are indicated by \* $p < .05$ , \*\* $p < .01$ , \*\*\* $p < .001$  (unpaired Student's  $t$ -test).

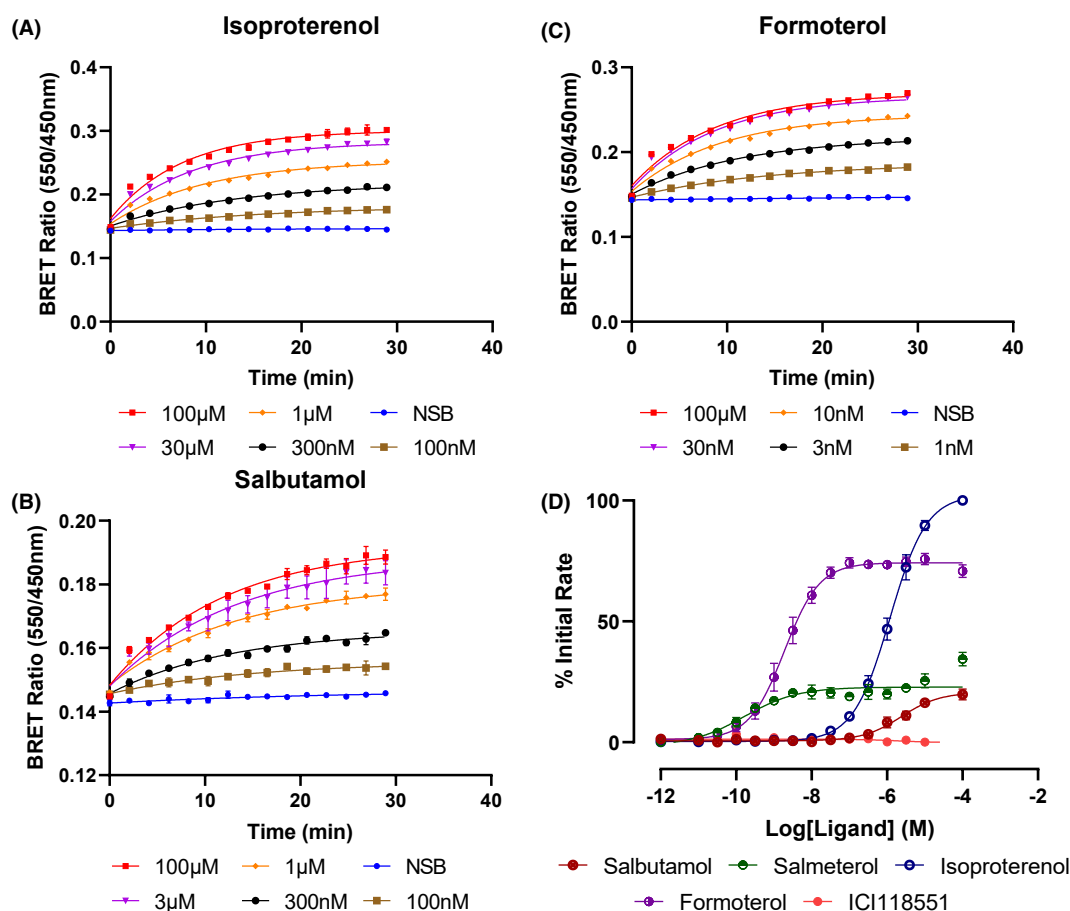


**FIGURE 4** The kinetics of TMR-G $\alpha$ s19cha18 stimulated recruitment to the  $\beta_2$ -AR. (A–C) show the concentration-dependent time courses of TMR-G $\alpha$ s19cha18 recruitment measured by NanoBRET in HBSS buffer. Data are representative examples from five independent experiments. (D) Initial rates of TMR-G $\alpha$ s19cha18 recruitment at each agonist concentration were calculated based on a rise to steady-state model, and plotted to generate the pooled concentration–initial rate curves. Normalized data from four independent experiments are shown, to the 100  $\mu$ M isoproterenol response.

### 3.5 | The TMR-G $\alpha$ s19cha18 binding assay as a detection method for ligands binding the GsGPCR G protein interaction site

To determine whether TMR-G $\alpha$ s19cha18 could be used as a tracer in binding studies to obtain rank orders of

affinity for putative IAMs, NanoBRET competition binding was performed in ss $\beta_2$ -AR-tsNluc membranes, using the candidate unlabeled G $\alpha$  C-terminal peptides G $\alpha$ s19cha18, G $\alpha$ s24, G $\alpha$ s11, and G $\alpha$ i24 (Table 1), in the presence of isoproterenol (Figure 6). Both G $\alpha$ s19cha18 and G $\alpha$ s24 successfully competed for the G protein binding site labeled by TMR-G $\alpha$ s19cha18, allowing derivation

Compounds	Endpoint		Kinetics rate	
	pEC <sub>50</sub> ± SEM (M)	R <sub>max</sub> ± SEM (%)	pEC <sub>50</sub> ± SEM (M)	R <sub>max</sub> ± SEM (%)
Salbutamol	5.91 ± 0.22	26.6 ± 3.4	5.66 ± 0.20	20.18 ± 2.34
Salmeterol	9.85 ± 0.21	32.4 ± 1.6	10.02 ± 0.34	22.28 ± 2.51
Isoproterenol	6.15 ± 0.09	101.1 ± 1.2	5.92 ± 0.10	102.5 ± 0.87
Formoterol	9.02 ± 0.21	78.0 ± 3.2	8.73 ± 0.16	74.1 ± 1.73
ICI118551	–	1.50 ± 1.4	–	1.21 ± 0.59

Note: Data are presented as mean ± SEM and are from four to five different experiments. Kinetic R<sub>max</sub> calculated as mean steady-state response at maximal concentration of ligand, Endpoint R<sub>max</sub> taken as response at maximal concentration of ligand.

TABLE 4 Agonist potencies and maximal responses derived from TMR-Gαs19cha18 binding using endpoint or kinetically derived data from high sodium experiments

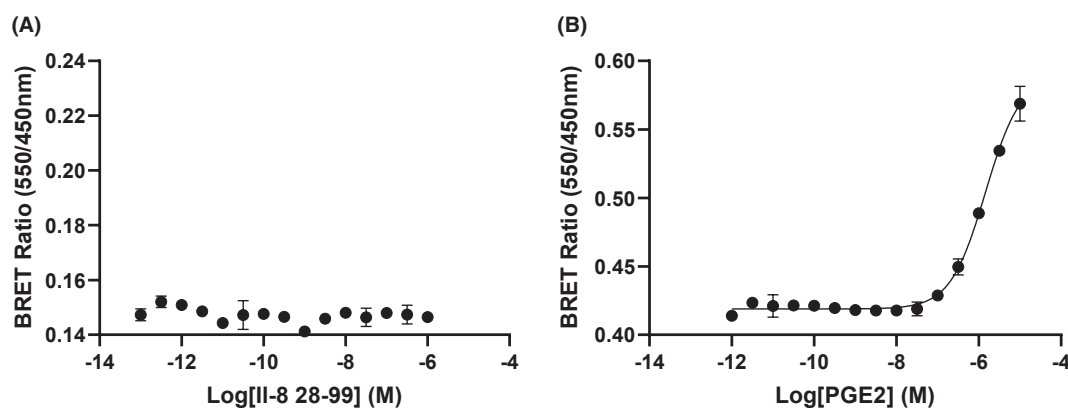


FIGURE 5 Agonist-induced TMR-Gαs19cha18 recruitment is also observed for the Gs-coupled EP<sub>2</sub> receptor but not the Gi-coupled CXCR2 receptor. (A) TMR-Gαs19cha18 NanoBRET measurements performed in ssCXCR2-tSNLuc membranes in the absence or presence of the chemokine CXCL8 (30 min). (B) Recruitment of TMR-Gαs19cha18 to EP<sub>2</sub>-tSNLuc measured by NanoBRET after PGE<sub>2</sub> stimulation (30 min). For each receptor, data represent an individual duplicate experiment displaying mean ± SD, from three performed.

of their respective affinities (Gαs19cha18 > Gαs24). The determined K<sub>i</sub> for unlabeled Gαs19cha18 (249 ± 38 nM, *n* = 5) was equivalent to that directly measured for the TMR-Gαs19cha18 probe. In contrast, Gαs11 and Gαi24 did not display any detectable competition with the tracer peptide, even with a reduction in tracer concentration (Figure S6), supporting the predicted order of selectivity of the different peptides for α5 helix binding site for Gs-coupled receptors.

## 4 | DISCUSSION

The development of selective therapeutics targeting Class A GPCRs can be limited by inherent structural homology between orthosteric binding sites for related receptor subtypes, and in this context, allosteric modulation provides an attractive alternative approach for drug discovery. Within this arena, a number of successful negative intracellular allosteric modulators (IAMs) have been generated that target the receptor–G protein effector interface to inhibit signaling,<sup>8,10–14</sup> a mechanism that in principle

should be broadly applicable to many GPCR families. The conformational selectivity of some IAMs may also be beneficial therapeutically, for example, in binding the active agonist-occupied GPCR conformation preferentially to generate use dependence.<sup>1,9,35</sup> However, a universal route to studying and screening the G protein IAM binding site has been more challenging to identify. Here, we show that Gα C-terminal peptides, which have been previously reported to act as intracellular allosteric modulators of GPCR signaling,<sup>16–18,20,21,36</sup> can be used as a basis to generate novel fluorescent probes for the G protein/IAM binding site, and to establish a real-time, resonance energy transfer biosensor assay for binding. We demonstrate that our candidate peptide tracer acts as a novel quantitative detector of Gs receptor activation by agonists and allows the development of a binding assay suitable for screening, to directly determine the affinities of competing IAM peptides and other modulators at this site.

The length, sequence, and likely conformation of Gα C-terminal peptides have previously been shown to be essential for demonstrating binding and allosteric effects on agonist affinity.<sup>21</sup> We first validated these findings for key

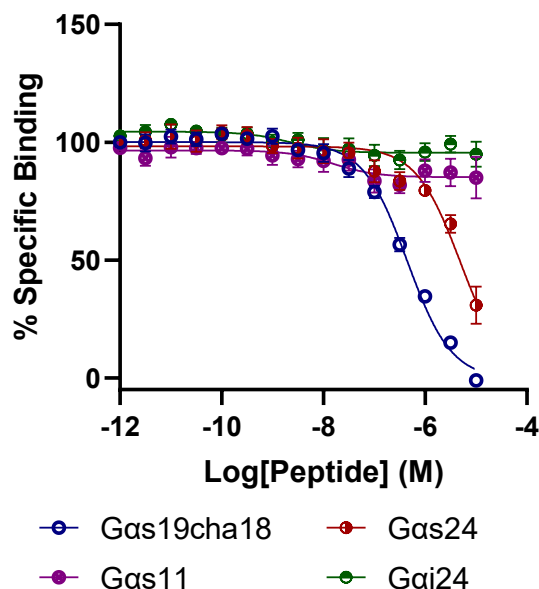


**FIGURE 6** NanoBRET competition binding assays using TMR-G $\alpha$ s19cha18 to affinities of unlabeled G $\alpha$  C terminal peptides for the ss $\beta_2$ -AR-tsNluc receptor in membranes. Assays were performed in low sodium buffer, for 2 h at 37°C using 500 nM fluorescent tracer. Data are pooled and normalized from five independent experiments.

peptides using a  $\beta_2$ -AR TR-FRET binding assay, using the orthosteric antagonist BODIPY-FL-propranolol<sup>24,32</sup> as the fluorescent probe. Use of a membrane assay format also allowed candidate peptides unrestricted access to the  $\beta_2$ -AR intracellular surface. Although shorter C terminal G $\alpha$  peptides have previously been reported to be functionally active,<sup>17,18,20</sup> our binding assay did not detect an ability of the 11 amino acid G $\alpha$ s11 to influence orthosteric ligand binding at the  $\beta_2$ -AR. However, extension of the C terminal sequence to 24 amino acids in G $\alpha$ s24 revealed its allosteric effect, in increasing  $\beta_2$ -AR agonist affinity. This may be due to the increased stability of the G $\alpha$ s peptide secondary structure produced by additional predicted  $\alpha$ -helical turns, giving greater structural homology to the native G protein  $\alpha 5$  helix. As reported by Mannes et al.,<sup>21</sup> substitution of the penultimate leucine residue for a cyclohexylalanine residue in the 19 amino G $\alpha$ s19cha18 generated a peptide with the greatest allosteric effects. The affinity shift observed with G $\alpha$ s19cha18 was only observed with the orthosteric agonists tested, and greatest for high efficacy agonists formoterol and isoproterenol (compared to lower efficacy salbutamol)—in line with the predictions of the ternary complex model relating orthosteric agonist efficacy to the magnitude of agonist affinity changes for uncoupled and G protein-coupled receptor complexes.<sup>37</sup> These data confirm that cha substitution in the penultimate position of the G $\alpha$ s C terminal sequence appears beneficial for its interactions with the  $\beta_2$ -AR G protein  $\alpha 5$

helix binding pocket sensed by the lower ends of TM3 and TM5.<sup>7</sup>

Using G $\alpha$ s19cha18 as a template, we then generated a new TMR-labeled fluorescent probe to be used in conjunction with C terminal nanoluciferase fused GPCRs in NanoBRET binding assays.<sup>22,23,25,38</sup> The use of BRET methodology, like TR-FRET, allows for the measurement of tracer recruitment with a high signal to noise ratio, and in a homogeneous assay format without separation of the bound and free ligand. Thus, it provides the opportunity to probe ligand binding kinetics as well as equilibrium measurements at the IAM G protein binding site.<sup>22,24,25</sup>

TMR-G $\alpha$ s19cha18 saturation studies using TMR-G $\alpha$ s19cha18 binding to  $\beta_2$ -AR-Nluc membranes demonstrated clear specific binding to the receptor detected by NanoBRET, exclusively in the presence of isoproterenol agonist. These data confirm the reciprocal allosteric effects between orthosteric agonist, active receptor confirmation, and the G mimetic peptides engaging the intracellular binding site,<sup>37</sup> illustrating the use-dependent mechanism of these probes and related G protein mimetic peptides, in which binding is enhanced by receptor stimulation with orthosteric ligands. The measured  $K_D$  ( $599 \pm 25$  nM) of TMR-G $\alpha$ s19cha18 was somewhat lower than that reported by Mannes et al. for the unlabeled peptide in radioligand binding studies,<sup>21</sup> differences that may result from the level of receptor expression in the insect sf9 cell system<sup>21</sup> compared to our human HEK293 cell approach. We did not observe the modification of TMR-G $\alpha$ s19cha18 binding with inclusion of nonhydrolyzable GTP analogs in the assay buffer, which might be predicted to disrupt  $\beta_2$ -AR interaction with native membrane G proteins (data not shown).

The use-dependent behavior of the TMR-G $\alpha$ s19cha18 probe enabled its application as a signaling biosensor to discriminate orthosteric agonist efficacies at the  $\beta_2$ -AR, focussing directly on receptor conformational change to the active conformation and so excluding amplification effects from downstream signaling readouts. TMR-G $\alpha$ s19cha18 recruitment assays defined potencies and maximal responses (full/partial), for example, representative agonists of differing efficacy, in a manner comparable to previous findings.<sup>39</sup> The effect of high sodium concentration, as a known negative allosteric modulator of class A GPCR conformational change to an active state,<sup>40,41</sup> demonstrated a predicted decrease in agonist potency, and enhanced the partial agonism (reduced  $R_{max}$ ) apparent for those ligands (salmeterol, salbutamol) with lower intrinsic efficacy. Notably, the assay enabled simple collection of kinetic TMR-G $\alpha$ s19cha18 recruitment data and analysis of agonist pharmacology using initial TMR-G $\alpha$ s19cha18 rates of association,<sup>34</sup> providing the opportunity to routinely monitor time

dependent, as well as equilibrium agonist behavior in one plate format.

The advantages of the TMR-G $\alpha$ s19cha18 biosensor in part derive from a relatively modest affinity and rapid binding kinetics, expected to follow changes in receptor conformation faithfully during activation. This may prove beneficial compared to previously reported sensors that detect the active receptor conformation with very high affinity, including miniG proteins or Nb80 nanobody recruitment, or where the sensor is tethered in close proximity to the G protein binding site through fusion to the receptor C terminus (e.g., SPASM sensors).<sup>42,43</sup> Moreover, the testing of the Gs-coupled EP<sub>2</sub> receptor or Gi-coupled CXCR2 within this system demonstrated TMR-G $\alpha$ s19cha18's ability to bind selectively to distinct Gs-coupled receptors  $\beta_2$ -AR and EP<sub>2</sub>, but not to CXCR2. The ability of TMR-G $\alpha$ s19cha18 to bind to further Gs-selective GPCRs is outside the scope of this study; however, given the shared homology with the native alpha-subunit  $\alpha_5$  helix, these initial findings indicate the potential for such probes to recognize the G protein binding sites of a variety of Gs-coupled receptors.

A key application of TMR-G $\alpha$ s19cha18 NanoBRET assays would be the ability to directly determine the affinities of unlabeled ligands at the G protein binding site through competition analysis, for example, in the identification of new lead molecules for IAMs. Previously, such studies have only been achieved through the generation of specific radioligand IAM probes for particular receptors, such as CXCR2.<sup>44</sup> As a proof of concept, a NanoBRET competition binding format was established for  $\beta_2$ -AR-Nluc (in the presence of saturating concentrations of isoproterenol). This allowed quantitative affinity estimation for the unlabeled peptides G $\alpha$ s19cha18 and G $\alpha$ s24, and confirmed the lack of affinity of G $\alpha$ s11 and G $\alpha$ i24 for the  $\beta_2$ -AR intracellular site—dovetailing with the indirect measurements of their action on orthosteric agonist binding. One consequence of the observed probe selectivity for the agonist-occupied receptor conformation is that in future screening efforts, such binding assays are likely to reveal negative allosteric modulators with a preference for the receptor active state, which would provide them with a use-dependent mode of action.<sup>14</sup> This provides an additional route for therapeutic selectivity by allowing therapeutic targeting to particular regions (e.g., CNS synapses) where the target receptors are highly active, avoiding a more general inhibitory profile that might lead to undesired on target effects.

Overall, our findings demonstrate that novel G $\alpha$ s mimetic fluorescent probes, in combination with receptor NanoBRET technology, provide a broad strategy to

monitor activation-dependent changes and binding to GsPCR intracellular modulator sites. Such biosensors provide new real-time readouts for orthosteric agonist activation and quantification of agonist efficacy, as well as the ability to establish NanoBRET competition binding assays to screen candidate use-dependent IAMs in a medium throughput format.

## AUTHOR CONTRIBUTIONS

James P. Farmer, Nicholas D. Holliday, Shailesh N. Mistry, and Charles A. Laughton designed the experiments and wrote the manuscript. James P. Farmer performed and analyzed the experiments.

## ACKNOWLEDGMENTS

This work was funded by The British Pharmacological Society AJ Clark studentship. The authors would like to thank Dr Desislava Nesheva for supplying CXCR2 cell membranes and Dr Nicola Dijon for providing initial EP<sub>2</sub> constructs.

## DISCLOSURES

The authors declare that there is no conflict of interest regarding the publication of this article.

## DATA AVAILABILITY STATEMENT

The data that support the findings of this study are available on request from the corresponding authors.

## ORCID

James P. Farmer  <https://orcid.org/0000-0002-4224-9299>

Shailesh N. Mistry  <https://orcid.org/0000-0002-2252-1689>

Charles A. Laughton  <https://orcid.org/0000-0003-4090-3960>

Nicholas D. Holliday  <https://orcid.org/0000-0002-2900-828X>

## REFERENCES

- Rosenbaum DM, Rasmussen SGF, Kobilka BK. The structure and function of G-protein-coupled receptors. *Nature*. 2009;459(7245):356-363. doi:10.1038/nature08144
- Weis WI, Kobilka BK. Structural insights into G-protein-coupled receptor activation. *Curr Opin Struct Biol*. 2008;18(6):734-740. doi:10.1016/j.sbi.2008.09.010
- Alexander S, Mathie A, Peters J. Guide to receptors and channels (GRAC), 5<sup>o</sup> Ed. *Br J Pharmacol*. 2011;164:S1-S2. doi:10.1109/ISCAS.2009.5118218
- Flock T, Hauser AS, Lund N, Gloriam DE, Balaji S, Babu MM. Selectivity determinants of GPCR-G-protein binding. *Nature*. 2017;545(7654):317-322. doi:10.1038/nature22070
- Stott LA, Hall DA, Holliday ND. Unravelling intrinsic efficacy and ligand bias at G protein coupled receptors: a practical guide

- to assessing functional data. *Biochem Pharmacol.* 2016;101:1-12. doi:10.1016/j.bcp.2015.10.011
6. Syrovatkina V, Alegre KO, Dey R, Huang XY. Regulation, signaling, and physiological functions of G-proteins. *J Mol Biol.* 2016;428:3850-3868. doi:10.1016/j.jmb.2016.08.002
  7. Rasmussen SGF, Devree BT, Zou Y, et al. Crystal structure of the  $\beta$  2 adrenergic receptor-Gs protein complex. *Nature.* 2011;477:549-555. doi:10.1038/nature10361
  8. Liu X, Ahn S, Kahsai AW, et al. Mechanism of intracellular allosteric  $\beta$ 2AR antagonist revealed by X-ray crystal structure. *Nature.* 2017;548(7668):480-484. doi:10.1038/nature23652
  9. Qu C, Mao C, Xiao P, et al. Ligand recognition, unconventional activation, and G protein coupling of the prostaglandin E2 receptor EP2 subtype. *Sci Adv.* 2021;7(14):eabf1268. doi:10.1126/SCIADV.ABF1268/SUPPL\_FILE/ABF1268\_SM.PDF
  10. Andrews G, Jones C, Wreggett KA. An intracellular allosteric site for a specific class of antagonists of the CC chemokine G protein-coupled receptors CCR4 and CCR5. *Mol Pharmacol.* 2008;73(3):855-867. doi:10.1124/mol.107.039321
  11. Nicholls DJ, Tomkinson NP, Wiley KE, et al. Identification of a putative intracellular allosteric antagonist binding-site in the CXC chemokine receptors 1 and 2. *Mol Pharmacol.* 2008;74(5):1193-1202. doi:10.1124/mol.107.044610
  12. Gonsiorek W, Fan X, Hesk D, et al. Pharmacological characterization of Sch527123, a potent allosteric CXCR1/CXCR2 antagonist. *J Pharmacol Exp Ther.* 2007;322(2):477-485. doi:10.1124/jpet.106.118927
  13. Lu H, Yang T, Xu Z, et al. Discovery of novel 1-cyclopentenyl-3-phenylureas as selective, brain penetrant, and orally bioavailable CXCR2 antagonists. *J Med Chem.* 2018;61:2518-2532. doi:10.1021/acs.jmedchem.7b01854
  14. Jiang C, Amaradhi R, Ganesh T, Dingleline R. An agonist dependent allosteric antagonist of prostaglandin EP2 receptors. *ACS Chem Neurosci.* 2020;11(10):1436-1446. doi:10.1021/ACSCHEMNEURO.0C00078/SUPPL\_FILE/CN0C00078\_SI\_001.PDF
  15. Scholten D, Canals M, Maussang D, et al. Pharmacological modulation of chemokine receptor function. *Br J Pharmacol.* 2012;165(6):1617-1643. doi:10.1111/j.1476-5381.2011.01551.x
  16. Hamm HE, Deretic D, Arendt A, Hargrave PA, Koenig B, Hofmann KP. Site of G protein binding to rhodopsin mapped with synthetic peptides from the  $\alpha$  subunit. *Science.* 1988;241(4867):832-835. doi:10.1126/science.3136547
  17. Rasenick MM, Watanabe M, Lazarevic MB, Hatta S, Hamm HE. Synthetic peptides as probes for G protein function. Carboxyl-terminal G alpha s peptides mimic Gs and evoke high affinity agonist binding to beta-adrenergic receptors. *J Biol Chem.* 1994;269(34):21519-21525. doi:10.1016/S0021-9258(17)31835-5
  18. Gilchrist A, Li A, Hamm HE. G COOH-terminal minigene vectors dissect heterotrimeric G protein signaling. *Sci Signal.* 2002;2002(118):pl1. doi:10.1126/scisignal.1182002pl1
  19. Gilchrist A, Bünemann M, Li A, Hosey MM, Hamm HE. A dominant-negative strategy for studying roles of G proteins in vivo. *J Biol Chem.* 1999;274(10):6610-6616. doi:10.1074/jbc.274.10.6610
  20. Gilchrist A, Vanhauwe JF, Li A, Thomas TO, Voyno-Yasenetskaya T, Hamm HE. G $\alpha$  minigenes expressing C-terminal peptides serve as specific inhibitors of thrombin-mediated endothelial activation. *J Biol Chem.* 2001;276(28):25672-25679. doi:10.1074/jbc.M100914200
  21. Mannes M, Martin C, Triest S, et al. Development of generic G protein peptidomimetics able to stabilize active state Gs protein-coupled receptors for application in drug discovery. *Angew Chem Int Ed.* 2021;60(18):10247-10254. doi:10.1002/anie.202100180
  22. Stoddart LA, Kilpatrick LE, Hill SJ. NanoBRET approaches to study ligand binding to GPCRs and RTKs. *Trends Pharmacol Sci.* 2018;39(2):136-147. doi:10.1016/j.tips.2017.10.006
  23. Soave M, Briddon SJ, Hill SJ, Stoddart LA. Fluorescent ligands: bringing light to emerging GPCR paradigms. *Br J Pharmacol.* 2020;177(5):978-991. doi:10.1111/bph.14953
  24. Sykes DA, Stoddart LA, Kilpatrick LE, Hill SJ. Binding kinetics of ligands acting at GPCRs. *Mol Cell Endocrinol.* 2019;485:9-19. doi:10.1016/j.mce.2019.01.018
  25. Stoddart LA, White CW, Nguyen K, Hill SJ, Pflieger KDG. Fluorescence- and bioluminescence-based approaches to study GPCR ligand binding. *Br J Pharmacol.* 2016;173(20):3028-3037. doi:10.1111/bph.13316
  26. Sykes DA, Moore H, Stott L, et al. Extrapyramidal side effects of antipsychotics are linked to their association kinetics at dopamine D2 receptors. *Nat Commun.* 2017;8(1):763. doi:10.1038/s41467-017-00716-z
  27. Baker JG, Adams LA, Salchow K, et al. Synthesis and characterization of high-affinity 4,4-difluoro-4-bora-3a,4a-diaza-s-indacene-labeled fluorescent ligands for human  $\beta$ -adrenoceptors. *J Med Chem.* 2011;54(19):6874-6887. doi:10.1021/JM2008562
  28. Valentin-Hansen L, Groenen M, Nygaard R, Frimurer TM, Holliday ND, Schwartz TW. The arginine of the DRY motif in transmembrane segment III functions as a balancing micro-switch in the activation of the  $\beta$ 2-adrenergic receptor. *J Biol Chem.* 2012;287(38):31973-31982. doi:10.1074/JBC.M112.348565
  29. Hoare BL, Kaur A, Harwood CR, et al. Measurement of non-purified GPCR thermostability using the homogeneous ThermoBRET assay. *bioRxiv.* 2020;2020.08.05.237982. doi:10.1101/2020.08.05.237982
  30. Dixon AS, Schwinn MK, Hall MP, et al. NanoLuc complementation reporter optimized for accurate measurement of protein interactions in cells. *ACS Chem Biol.* 2016;11(2):400-408. doi:10.1021/acscchembio.5b00753
  31. Baker JG. The selectivity of  $\beta$ -adrenoceptor antagonists at the human  $\beta$ 1,  $\beta$ 2 and  $\beta$ 3 adrenoceptors. *Br J Pharmacol.* 2005;144(3):317-322. doi:10.1038/sj.bjp.0706048
  32. Sykes DA, Charlton SJ. Single step determination of unlabeled compound kinetics using a competition association binding method employing time-resolved FRET. *Methods Mol Biol.* 2018;1824:177-194. doi:10.1007/978-1-4939-8630-9\_10
  33. Sykes DA, Charlton SJ. Slow receptor dissociation is not a key factor in the duration of action of inhaled long-acting  $\beta$ 2-adrenoceptor agonists. *Br J Pharmacol.* 2012;165(8):2672-2683. doi:10.1111/J.1476-5381.2011.01639.X
  34. Hoare SRJ, Tewson PH, Quinn AM, Hughes TE, Bridge LJ. Analyzing kinetic signaling data for G-protein-coupled receptors. *Sci Rep.* 2020;10(1):1-23. doi:10.1038/s41598-020-67844-3
  35. Hilger D, Masureel M, Kobilka BK. Structure and dynamics of GPCR signaling complexes. *Nat Struct Mol Biol.* 2018;25(1):4-12. doi:10.1038/S41594-017-0011-7

36. Mazzoni MR, Taddei S, Giusti L, et al. A G $\alpha$ (s) carboxyl-terminal peptide prevents G(s) activation by the A(2A) adenosine receptor. *Mol Pharmacol*. 2000;58(1):226-236. doi:10.1124/mol.58.1.226
37. de Lean A, Stadel JM, Lefkowitz RJ. A ternary complex model explains the agonist-specific binding properties of the adenylate cyclase-coupled beta-adrenergic receptor. *J Biol Chem*. 1980;255(15):7108-7117. doi:10.1016/S0021-9258(20)79672-9
38. Stoddart LA, Johnstone EKM, Wheal AJ, et al. Application of BRET to monitor ligand binding to GPCRs. *Nat Methods*. 2015;12(7):661-663. doi:10.1038/NMETH.3398
39. Dijon NC, Nesheva DN, Holliday ND, Aires S, Martins M, Miguel D. Luciferase complementation approaches to measure GPCR signaling kinetics and bias. *Methods Mol Biol*. 2021;2268:249-274. doi:10.1007/978-1-0716-1221-7\_17
40. Katritch V, Fenalti G, Abola EE, Roth BL, Cherezov V, Stevens RC. Allosteric sodium in class A GPCR signaling. *Trends Biochem Sci*. 2014;39(5):233-244. doi:10.1016/J.TIBS.2014.03.002
41. Agasid MT, Sørensen L, Urner LH, Yan J, Robinson CV. The effects of sodium ions on ligand binding and conformational states of G protein-coupled receptors-insights from mass spectrometry. *J Am Chem Soc*. 2021;143(11):4085-4089. doi:10.1021/JACS.0C11837/ASSET/IMAGES/LARGE/JA0C11837\_0002.JPEG
42. Wan Q, Okashah N, Inoue A, et al. Mini G protein probes for active G protein-coupled receptors (GPCRs) in live cells. *J Biol Chem*. 2018;293(19):7466-7473. doi:10.1074/jbc.RA118.001975
43. Kim K, Paulekas S, Sadler F, et al.  $\beta$ 2-adrenoceptor ligand efficacy is tuned by a two-stage interaction with the G $\alpha$ s C terminus. *Proc Natl Acad Sci*. 2021;118(11):e2017201118. doi:10.1073/pnas.2017201118
44. Salchow K, Bond M, Evans S, et al. A common intracellular allosteric binding site for antagonists of the CXCR2 receptor: research paper. *Br J Pharmacol*. 2010;159:1429-1439. doi:10.1111/j.1476-5381.2009.00623.x

## SUPPORTING INFORMATION

Additional supporting information can be found online in the Supporting Information section at the end of this article.

**How to cite this article:** Farmer JP, Mistry SN, Laughton CA, Holliday ND. Development of fluorescent peptide G protein-coupled receptor activation biosensors for NanoBRET characterization of intracellular allosteric modulators. *The FASEB Journal*. 2022;36:e22576. doi: [10.1096/fj.202201024R](https://doi.org/10.1096/fj.202201024R)